Environmental Science & Technology

Article

pubs.acs.org/est

Tracking and Quantification of Single-Walled Carbon Nanotubes in Fish Using Near Infrared Fluorescence

Joseph H. Bisesi, Jr.,[†] Jonathan Merten,[‡,◆] Keira Liu,[§,#] Ashley N. Parks,[∥,#,¶] A. R. M. Nabiul Afrooz,[∇,□] J. Brad Glenn,[○] Stephen J. Klaine,[○] Andrew S. Kane,[†] Navid B. Saleh,[∇,□] P. Lee Ferguson,[∥,⊥,#] and Tara Sabo-Attwood[†,*]

[†]Department of Environmental and Global Health, Center for Environmental and Human Toxicology, University of Florida, 2187 Mowry Road, Box 110885, Gainesville, Florida 32611, United States

[‡]Department of Chemistry, University of Florida, 214 Leigh Hall, Box 117200, Gainesville, Florida 32611, United States

[§]Department of Chemistry, Duke University, 124 Science Drive, Box 90354, Durham, North Carolina 27708, United States

[#]Center for the Environmental Implications of Nanotechnologies (CEINT), Duke University, 121 Hudson Hall, Box 90287, Durham, North Carolina 27708, United States

[∥]Nicholas School of the Environment, Duke University, Box 90328, Durham, North Carolina 27708, United States

[∇]Department of Civil and Environmental Engineering, University of South Carolina, 300 Main Street, Columbia, South Carolina 29208, United States

[○]Institute of Environmental Toxicology, Department of Biological Sciences, Clemson University, 509 Westinghouse Road, Box 709, Pendleton, South Carolina 29670, United States

[⊥]Department of Civil and Environmental Engineering, Duke University, 121 Hudson Hall, Box 90287, Durham, North Carolina 27708, United States

ABSTRACT: Detection of SWCNTs in complex matrices presents a unique challenge as common techniques lack spatial resolution and specificity. Near infrared fluorescence (NIRF) has emerged as a valuable tool for detecting and quantifying SWCNTs in environmental samples by exploiting their innate fluorescent properties. The objective of this study was to optimize NIRF-based imaging and quantitation methods for tracking and quantifying SWCNTs in an aquatic vertebrate model in conjunction with assessing toxicological end points. Fathead minnows (*Pimephales promelas*) were exposed by single gavage to SWCNTs and their distribution was tracked using a custom NIRF imaging system for 7 days. No overt toxicity was observed in any of the SWCNT treated fish; however, histopathology observations from gastrointestinal (GI) tissue revealed edema within the submucosa and altered mucous cell morphology. NIRF images showed strong SWCNT-derived fluorescence signals in whole fish and excised intestinal tissues. Fluorescence was not detected in other tissues examined, indicating that no appreciable intestinal absorption occurred. SWCNTs were quantified in intestinal tissues using a NIRF spectroscopic method revealing values that were consistent with the pattern of fluorescence observed with NIRF imaging. Results of this work demonstrate the utility of NIRF imaging as a valuable tool for examining uptake and distribution of SWCNTs in aquatic vertebrates.

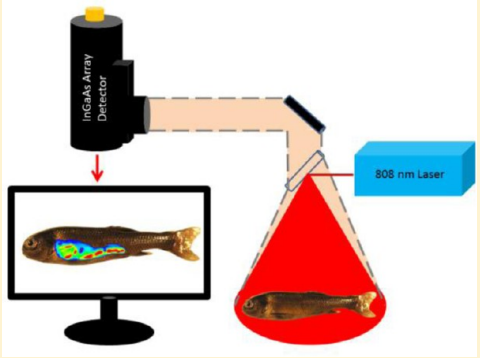

INTRODUCTION

Single walled carbon nanotubes (SWCNTs) are a highly ordered allotrope of black carbon exhibiting strong covalent (sp^2) bonding between carbon atoms and structural and electronic properties most similar to graphite or diamond. Individual SWCNTs typically have a diameter in the range of 0.5−2 nm and are characterized by their high tensile strength, aspect ratio, and tunable electrical conductivity.[1] These unique characteristics have led to increased use in manufacturing and biomedical applications, yet the potential adverse health effects these materials may pose are not well understood.[2,3]

Much of the research on potential adverse health effects of SWCNTs has focused on mammalian health end points with a robust investigation of inhalation as a primary route of exposure.[4−6] Fewer studies have probed the toxicity associated with SWCNT exposure to aquatic organisms and the majority of these have focused on bacterial and invertebrate models. These reports reveal that SWCNTs can inactivate bacteria commonly found in wastewater treatment plants[7] and decrease survival of *Daphnia magna*[8] and the copepod *Amphiascus tenuiremis*.[2] Only a handful of studies have investigated effects

Received: October 14, 2013
Revised: December 20, 2013
Accepted: January 2, 2014
Published: January 2, 2014

 © 2014 American Chemical Society

on aquatic vertebrates, namely fish, and demonstrate that SWCNTs can impact reactive oxygen species production,[9,10] immune responses,[11] hatching success,[12] and modulate biomarkers of oxidative stress and gill pathology.[13]

A limitation inherent to investigating effects of carbon-based nanomaterials is our restricted ability to effectively assess their distribution in exposed animals. Unfortunately, traditional analytical methods for nanoparticles are relatively poorly suited for differentiating nanosized carbon materials from the carbon that comprises most of the biomass of living cells.[14] Some researchers have applied techniques such as transmission electron microscopy (TEM), Raman spectroscopy, fluorescent tagging, thermogravimetric analysis, size exclusion chromatography, and absorbance measurements in attempts to localize SWCNTs in vivo; but each of these techniques has limitations.[15−19] For example, Edgington et al.[15] used high resolution TEM and Raman spectroscopy to qualitatively assess SWCNT distribution in *Daphia magna* but were unable to differentiate these nanomaterials in tissues due to low contrast and lack of quantitative methods established for carbon. This poses a major challenge in advancing our understanding of carbon nanoparticle health impacts and highlights the crucial need for the development of superior methods for qualitative and quantitative measurements of SWCNT detection and distribution in complex biological samples.

Depending on the particular chiral graphene sheet wrapping vector (n,m) inherent to each SWCNT isoform, SWCNTs exhibit particular allowed and disallowed electronic transitions leading to classification as either semiconducting or metallic.[20] When excited with 600−800 nm wavelength light, individualized, pristine semiconducting SWCNTs in suspension exhibit native and intense fluorescence emission in the near-infrared (NIR) range due to electronic transitions across a semiconductor bandgap after excitation.[21,22] Their emission spectra thus reveal information about the structure of SWCNTs and can also be used to detect and quantify these materials in complex matrices. Fluorescence in the NIR region is especially valuable because biological systems exhibit little to no endogenous background fluorescence in this spectral range.[23] Additionally, these long excitation and emission wavelengths have lower extinction coefficients (due to scatter or absorption) than visible wavelengths, allowing high-quality imaging of nanotubes buried in several millimeters of tissue.[24] This has led investigators to consider the use of NIR fluorescence (NIRF) measurements to examine SWCNT interactions with biological systems without the need for molecular tagging. Recently, the principle of NIRF spectroscopy has been applied by members of our research team to develop a highly sensitive, quantitative method for quantifying SWCNTs in environmental and biological samples at nanogram levels.[25,26] High-resolution NIRF imaging methods have also been used in vitro to investigate ingestion of SWCNTs by phagocytic cells and to localize targeted cell receptors by utilizing the SWCNTs as fluorescent probes.[27,28] In vivo, SWCNTs fed to drosophila were identified in the malphighian tubules, salivary glands, brain, trachea, and fat bodies using NIRF imaging[29] and Welsher et al.[30,31] has demonstrated the utility of NIRF for deep tissue anatomical imaging in mice during intravenous injection. While this technology has been successful for the aforementioned applications, the use of NIRF spectroscopy and imaging in higher order aquatic vertebrates, organisms that are likely targets of exposure via water and food routes, has not been performed to date.

Aquatic environments may act as a sink for nanoparticulate contaminants such as SWCNTs,[32] therefore development of sensitive methods for tracking these agents in aquatic matrices is essential for assessing the biological effects of nanomaterials. The primary goal of the current research was to expand the use of NIRF imaging and spectroscopy methods to examine SWCNT distribution in fish. To accomplish this goal, we have constructed and optimized a custom NIRF imaging system that allows us to track real-time presence and distribution of SWCNTs via imaging of whole organisms and individual organs and tissues. As an initial proof of concept approach, oral gavage was used to simulate foodborne exposure in the fathead minnow (*Pimephales promelas*). Chirally enriched, predominantly semiconductive (6,5) SWCNTs, characterized by electron microscopy and light scattering, were used for the exposure. Distribution analysis via NIRF imaging was coupled with quantification of SWCNT in homogenized individual organs using NIRF spectroscopy methodologies.[25,26] Histology and transmission electron microscopy of the gastrointestinal tract were also employed to examine potential alterations at the tissue and cellular level.

■ MATERIALS AND METHODS

Suspension Preparation. Single-walled carbon nanotubes were graciously donated by SouthWest Nano-Technologies (Norman, OK) in dry form. SWCNT solutions were freshly prepared from powdered nanotubes as a suspension in 0.5% gum arabic (Sigma Aldrich, St. Louis, MO) dissolved in nanopure water. Initially, 4 mg of SWCNTs were added to 4 mL gum arabic solution and mixed vigorously using a vortex mixer. The solution was then sonicated on ice for two 10 min intervals at 50% amplitude using a Branson 450 sonifier fitted with a $^1/_8$" diameter microtip probe. After sonication, the solution was centrifuged at 14 100 rpm for 5 min. The resulting supernatant was carefully collected and the final concentration of SWCNTs in solution was measured by near-infrared fluorescence spectroscopy as previously described.[25]

Metal Leaching From SWCNT Suspensions. To quantify total metal content, triplicate SWCNT samples (20 mg dry weight) were combusted in 50 mL quartz beakers (precleaned with 3 M trace metal grade hydrochloric acid for three days prior to air-drying in a cleanroom hood) at 550 °C for 12 h in an electric muffle furnace. After cooling, 1 mL of concentrated nitric acid and 3 mL of concentrated hydrochloric acid (both trace metal grade) were added to the ash for digestion. The samples were then refluxed at approximately 150 °C for 30 min using a hot plate. After digestion, the samples were then evaporated to dryness with continuous heating. The residual solids in each beaker were redissolved in 4 mL of mixed acid (2% nitric acid and 0.5% hydrochloric acid), and this solution was diluted 1:5 with the same acid solution. The samples (5 mL) were then analyzed for a suite of trace elements by ICP-MS (Agilent 7700 quadrupole mass spectrometer) using internal calibration. Detection limits and sample recovery were assessed by concurrent analysis of trace elements in samples of NIST SRM 1643e (Trace Elements in Water).

For leaching experiments, SG65 SWCNTs were added to 1.5 mL of DMEM cell culture media at a final concentration of 50 μg/mL and incubated in the CO_2 incubator for 48 h. Incubation was carried out in properly cleaned (described above) glass vials. After 48 h of incubation, 1 mL from each sample were ultracentrifuged in properly cleaned tubes at 80 000 rpm for 30 min at 25 °C (Beckman Rotor, TLA-120.2). 3.

A total of 600 mL of the supernatant from each centrifuge tube was collected and transferred into 1.5 mL microcentrifuge tubes (properly cleaned as described above). The supernatants were stored at 4 °C for further metal analysis as described above.

Dynamic Light Scattering/Static Light Scattering. Dynamic light scattering (DLS) using a goniometer system (ALV-CGS/3, ALV-GmbH, Langen, Germany) was employed to evaluate stability of SWCNTs suspended in gum arabic (GA) solution over a 7 day period. A detailed measurement procedure has been described elsewhere.[33,34] In brief, 2 mL of 10 mg/L SWCNT sample was introduced to the sample chamber in a previously cleaned borosilicate vial (Fisher Scientific, Pittsburgh, PA). A 632.8 nm laser was shined through the sample and scattered light was collected at an angle of 90° in 15 s intervals for 1 h. Hydrodynamic radii (HR) of the nanoparticles were calculated by the software interface using the collected time-dependent scattering data. HRs of the particles were then plotted against measurement time to see the stability in this time period. This procedure was repeated after 6, 12, 24 h followed by a 24 h interval for 168 h to monitor changes in SWCNT aggregate size over the entire exposure period.

The ALV-CGS/3 goniometer system was also utilized to perform angle-dependent static light scattering (SLS) of GA suspended SWCNTs. Ten mg/L SWCNTs was added to a borosilicate glass vial and angle-dependent scattering was performed for an angular range of 12.5° to 100° with 0.5° increments. Fractal dimension was computed from log−log profiles of scattering intensity and wave vector. The slope of the fractal regime profile was then computed using linear fit, which represented the fractal dimension. Data were collected every 2 h for a 24 h duration. Further details of this method are described elsewhere.[35]

NIRF Imaging System. Excitation of samples was achieved with a Visotek 30 W, fiber coupled diode laser at 808 nm emission wavelength, set to 5 W output power (Visotek, Inc. Livonia, MI). The laser beam was reflected onto the sample with a 900 nm long-pass dichroic mirror (Thor Laboratories, Newton, NJ). Stokes-shifted emission was transmitted through the dichroic mirror, passed through two 1000 nm long-pass filters (Thor Laboratories, Newton, NJ), and finally imaged onto the detector by a 18−108 mm C mount zoom lens (Thor Laboratories, Newton, NJ). Emission was measured using a liquid nitrogen cooled Princeton Instruments OMA V InGaAs two-dimensional array detector (320 × 256 pixels) controlled by WinView Software (Princeton Instruments, Trenton, NJ). Please see the accompanying table of contents figure for a diagram of the NIRF imaging system.

NIRF images collected using the imaging system were exported to *x,y,z* matrix waves in Igor Pro 6.2 and processed for semiquantitative analysis. Specifically, the images were background subtracted (using a reference image containing no sample), smoothed (Savitsky-Golay 3 point algorithm), and thresholded (based on background pixel intensity). NIRF intensity at each pixel was evaluated and used to detect image "features" exhibiting significant SWCNT fluorescence. Such features were then defined and the outlines were used to create a mask for the processed image. Pixels within the feature mask were then intensity integrated to give an averaged intensity that could then be multiplied by the area (square pixels) to yield a fluorescence intensity value for each feature within a SWCNT-containing sample image. These intensity values for intestine samples were then used to evaluate total loss of SWCNT-derived NIRF signal over the course of the experimental time points.

NIRF Imaging System Detection Limits. There are many factors that influence the limit of detection (LOD) in our NIRF imaging system including image exposure time, laser power, laser wavelength, and tissue interactions. To provide a detection limit for the current study we chose to use the same settings as used for the fish images (808 nm laser @ 5W power, 1 s image exposure). Because dispersant plays a large role in fluorescence we conducted LOD experiments for 2% sodium deoxycholate (SDC), 1% pluronic F68, and 0.5% gum arabic. New suspensions in each of these dispersants were created as described above. A dilution series of each was prepared and imaged by placing a 10 μL aliquot on the sample platform. LOD was defined as the lowest concentration where discernible fluorescence was detected.

Fish Exposures. All animal studies were performed in accordance with the University of Florida Institutional Animal Care and Use Committee. Fathead minnows were bred and maintained at the Aquatic Toxicology Core Laboratory at the University of Florida. Fish were approximately 6 months old at the time of exposure (Mass: 1.70 ± 0.78g; Length: 55.6 ± 7 mm). Feed was withheld for four days prior to the initiation of the experiment to purge the intestines. On experiment day zero, fish were individually anesthetized using buffered MS-222 (Western Chemical Company, Ferndale, WA) and gavaged with 10 μL of SWCNT suspensions or 0.5% gum arabic depending on the treatment condition. Gavage was achieved by gently inserting a 10 μL pipet tip filled with suspension into the esophagus and carefully dispersing a 10 μL bolus it into the gut. NIRF images were taken before and immediately after gavage to visualize introduction of the SWCNTs to the GI tract. Fish were then placed in treatment- and time-point-specific holding tanks until sacrifice with MS-222. Fish were not fed during exposures. The mass, length, and gender of each fish was recorded, and light field and near-infrared images were acquired. Following whole fish imaging, internal organs were removed including intestine, liver, gonad, gall bladder, and spleen. Light field and near-infrared images were taken of the intact fish with the left "filet" removed, with and without organs, as well as all of the individual organs to examine distribution.

Experimental Design. Two separate experiments were conducted to examine distribution of SWCNTs in fish during GI exposures. For histological analysis and transmission electron microscopy (TEM), four fathead minnows were gavaged for each treatment and 2, 8, 24, 48, 96, and 168 h time points. The SWCNT treated fish were gavaged with 10 μL of a 318 μg/mL SWCNT in 0.5% gum arabic suspension and the control fish received 10 μL of 0.5% gum arabic. For SWCNT quantification in tissues, three fathead minnows were gavaged for each treatment and time point. Time points were 0, 2, 8, 24, 48, 96, and 168 h. The SWCNT treatment was gavaged with 10 μL of a 426 μg/mL SWCNT in 0.5% gum arabic suspension and the control treatment was gavaged with 10 μL of 0.5% gum arabic.

Transmission Electron Microscopy. Five to ten millimeter-long gut tract sections were dissected and placed into a 3.0% buffered glutaraldehyde (pH 7.1) solution overnight in 1.5 mL centrifuge tubes. After sections were fixed, they were rinsed in 0.2 M cacodylate buffer at pH 7.1 for 15 min and stepwise dehydrated in ethyl alcohol diluted with ultra pure water at 50, 70, 80, and 95% for 15 min and then 100% ethyl alcohol for 30

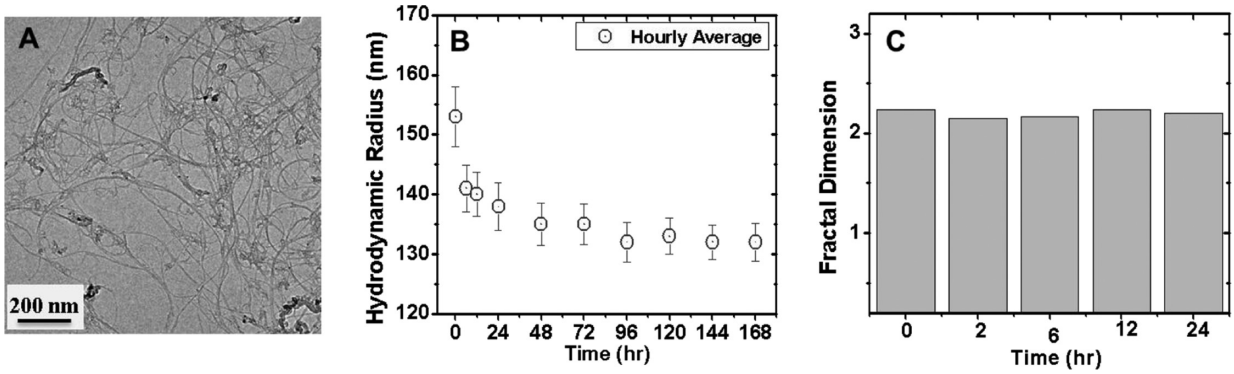

Figure 1. Particle characteristics of SWCNTs in suspension. (A) TEM images of dry SWCNTs before suspension revealed long filamentous and bundled particles; scale bar = 200 nm.(B) Suspensions used for gavage were diluted to 10 ug/mL with 0.5% gum arabic and particle size was measured over the exposure period at 25 °C using DLS. The aggregate mean size ranged from 153 to 132 nm. (C) Fractal dimension of particles in suspension over 24 h was measured by SLS and showed no change in fractal structures over time.

min. Sections were then rinsed with a 1:1 ethyl alcohol and L.R. white resin for 15 min on a nutating mixer. After rinsing with diluted resin, sections were placed into fresh L.R. white resin and placed back on the nutating mixer. After 15 min of mixing, sections were transferred into BEEM capsules with fresh L.R. White resin polymerization occurred at 60 °C in a drying oven overnight.

After the embedding process was complete, samples where sectioned using a DiATOME diamond knife on a Reichert Ultramicrotome, 90−100 nm thick, and captured on 200-mesh carbon Formvar copper grids (type FCF200-Cu). Microscopy samples were viewed on Hitachi 7600 TEM at 120 kV. Energy dispersive X-ray spectroscopy was performed on the Hitachi 4800SE at 25 kV with TE detector using Oxford instruments EDS/EDX detector (Clemson University Electron Microscope Facility).

Histology. The intact gastrointestinal tract from each fish was carefully dissected immediately upon sacrifice, positioned straight with fine needles on a piece of dental wax, and preserved in 10% neutral buffered formalin. Following preservation, each intestine was separated into four equally sized pieces, representing sections from proximal to distal. Sections were embedded in paraffin wax and cut in for routine histological processing.[36] Tissues were sectioned at 5 μM and sections were stained with hematoxylin and eosin for general tissue-level observations. Serial sections were stained with alcian blue/nuclear red counter stain to observe the number and relative size of mucin-positive cells.

SWCNT Quantification. Tissue concentrations of SWCNTs were measured using near-infrared fluorescence spectroscopy according to a previously published method [25] with modifications in sample preparation. Fish tissues (typically <50 mg wet) were suspended in 0.75 mL of SDC prior to ultrasonication (Branson Sonifier 450) using a 1/8" microtip probe at 50% amplitude for 10 min on ice. After a second round of sonication with an additional aliquot of SDC solution, the combined solution was transferred to a quartz cuvette and NIRF emission spectra were collected using an NS1 spectrofluorometer (Applied NanoFluorescence, Houston, TX) at three laser excitation wavelengths (638, 691, and 782 nm). Calibration was performed by five-point matrix-matched standard addition of SG65 SWCNTs to nonexposed fathead minnow intestinal tissue to account for any matrix effects on quantitation (e.g., internal filter effects or reduced recovery in extraction). SWCNT burdens were reported as mass SWCNT per fish.

■ RESULTS AND DISCUSSION

Assessment of the distribution and sublethal effects of carbon nanomaterials presents unique challenges that must be addressed to determine if these agents pose a significant risk to human and ecosystem health.[37] While routine methods exist for identifying various types of nanoparticles (e.g., metal oxides, TiO_2, quantum dots) in aquatic matrices, our current ability to track and quantify carbon-based materials is limited. Advanced imaging techniques are time-consuming and expensive and still lack in their ability to positively identify carbon nanomaterials in biological organisms.[15−19] The objective of this study was to enhance our capability to track SWCNTs in aquatic vertebrates by applying NIRF imaging and spectroscopy to the examination of SWCNT distribution in fish in conjunction with assessing toxicological end points.

SG65 SWCNTs are a well characterized mixture of primarily semiconductive (6,5) chirality-enriched, nonfunctionalized SWCNT formulation that has been used in a number of systematic environmental studies[25,26,34] These particular SWCNTs are produced by chemical vapor deposition method (specially termed CoMoCAT by the manufacturer SouthWest NanoTechnologies, Inc.) with >90% purity, and have an average diameter of 0.8 nm.[25] For the current study, we performed characterization of SWCNTs before and after suspension in 0.5% (w/v) gum Arabic dispersant solutions using TEM and dynamic and static light scattering (DLS and SLS) techniques. An example electron micrograph (Figure 1A) illustrates the presence of both filamentous and bundled SWCNTs. However, the micrographs did not show presence of significant metal catalysts, which are typically observed as dark and spherical entities in TEM imaging.[38] Our previous work has shown that the particular batch of SG65 SWCNTs used in this study contains <5% (w/w) metal catalyst (approximately 2:1 molybdenum:cobalt).[25] We additionally performed leaching experiments in cell culture media to represent a worst case scenario and results indicate that 3.8% and 0.93% (w/w) of the total cobalt and molybdenum, respectively, leached from the SWCNTs. For the highest dose used in this study, 4.26 μg of SWCNTs, the worst case scenario would be leaching of 8 ng and 2 ng of total cobalt and molybdenum, respectively. While these metals cannot be completely discounted as contributing to biological effects, the levels are quite low and well below

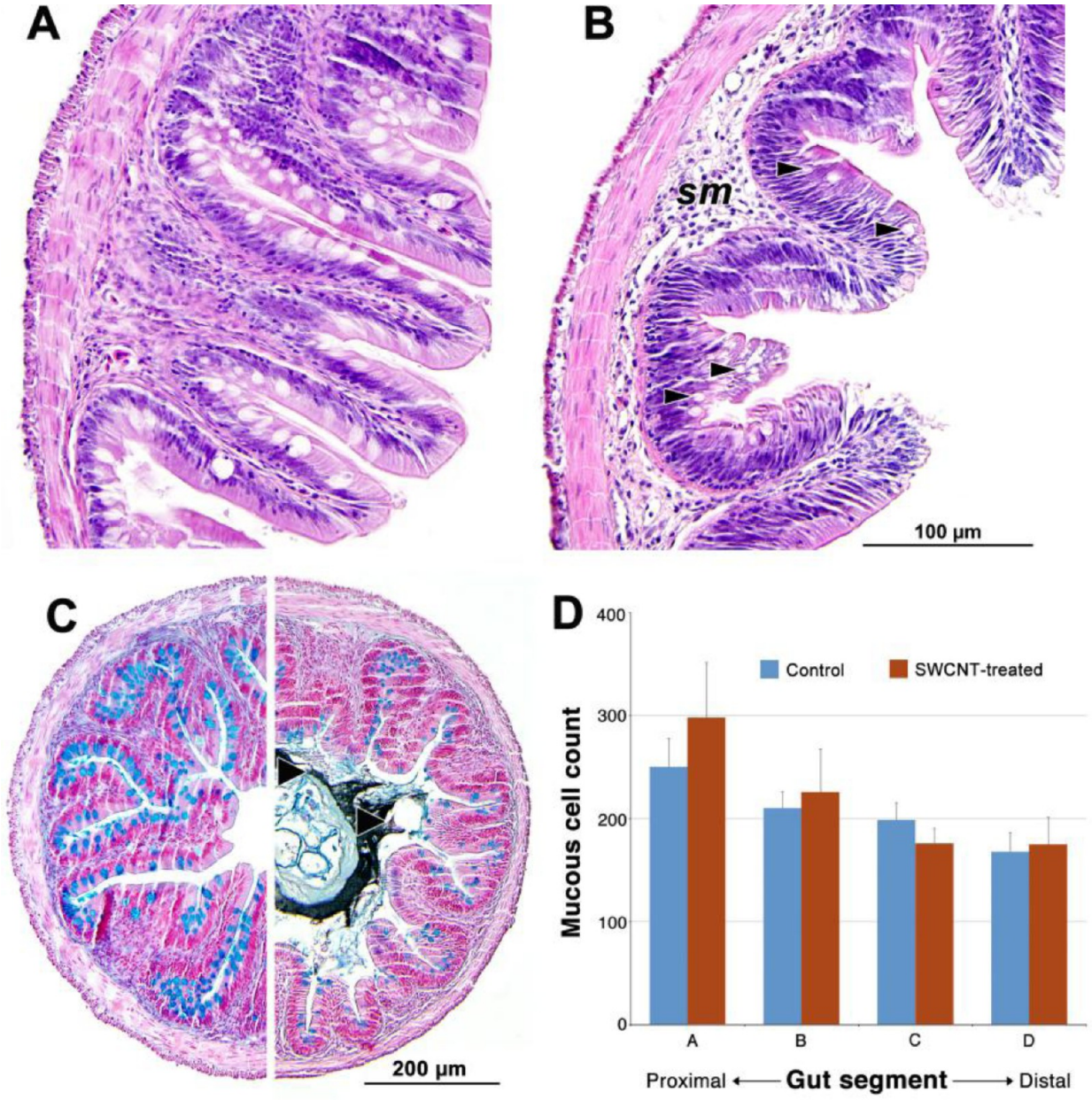

Figure 2. Histological sections of intestines from fish exposed to SWCNTs. H&E stained sections from (A) control and (B) SWCNT-treated fish showing mucous cell atrophy (arrowheads) and submucosal edema (sm) 24 h after treatment. (C) Alcian blue stained composite sections showing typical morphology of intestinal mucous cells in control fish (left) compared with mucus cell atrophy observed in SWCNT-treated fish (right) after 24 h. Also on the right, bolus of dark material associated with SWCNT exposure is seen within the lumen. (D) Mucin-positive cell counts in proximal and distal intestinal sections.

reported effect levels of cobalt (LC_{50}: 2.67−4.57 mg/L)[39] and molybdenum (LC_{50}: 577−678 mg/L)[39] in the fathead minnow.

To determine SWCNT aggregation state, gavage suspensions were diluted to 10 mg/L in 0.5% gum arabic and DLS was measured revealing an initial average cluster size of 153 nm that stabilized to 132 nm after 24 h (Figure 1B). It should be noted that that SWCNTs fold in suspension and form colloidal clusters and therefore the DLS measurement gives a measure of the average hydrodynamic radius of these clusters, rather than individual tubes.[33,34,40,41] Data provided by SLS analysis, measuring fractal dimension (D_f), showed moderately compact aggregates with D_f in the range of 2.2−2.3. The D_f also did not show any noticeable changes over the 24 h period (Figure 1C). These results imply that the SWCNTs maintain a relatively stable aggregate size and structure when suspended in gum arabic over time.

Fish were exposed to SWCNTs via a single gavage of 10 μL of the respective suspension for each experiment. NIRF imaging, quantitation, and histology analyses were performed at 2, 4, 8, 24, 48, 96, and 168 h. Exposure to SWCNTs did not cause any overt toxicity as we did not observe any impacts on viability and qualitative health throughout the study. To discern potential sublethal exposure effects at the tissue level, intestines were examined histologically for alterations in general architecture and cell morphology (Figure 2). Mild to moderate edema and vasodilation were observed in the intestinal submucosa (Figure 2B) of SWCNT treated fish relative to control fish (Figure 2A). Altered mucous cell morphology was

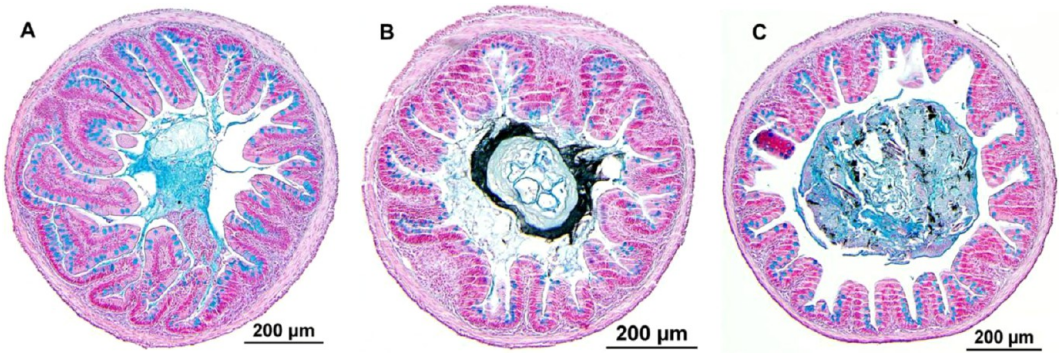

Figure 3. Histological cross sections of alcian blue stained intestinal tissue from (A) control and SWCNT treated fish after (B) 2 h and (C) 96 h. Note the dark bolus in the intestinal lumen of the SWCNT treated fish that is visible at 2 h and then becomes more dispersed and packaged by 96 h.

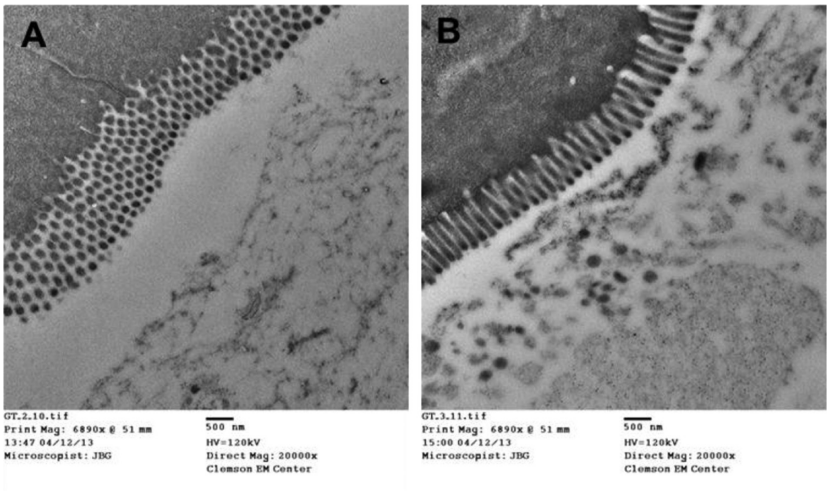

Figure 4. Transmission electron microscopy images of fathead minnow intestinal sections from (A) control and (B) SWCNT exposed fish. Electron micrographs were taken at 20,000x magnification; scale bar = 500 nm. Micrographs were focused on microvilli on an individual intestinal villus. Direct interactions with biological tissues were not observed throughout the exposure and SWCNTs could not be positively identified when compared to controls. Further attempts to identify particles using EDX analysis (not shown) did not reveal any catalyst metal signatures.

observed from alcian blue stained sections in SWCNT treated fish which can be interpreted as atrophy or massive mucus cell secretion compared with control fish (Figure 2C). We did not observe any obvious hypertrophy or reduction in the number of mucous cells between treatments in proximal and distal sections of intestine (Figure 2D). These specific effects have not been previously documented in fish exposed to SWCNTs to date however one other study with rainbow trout (*Onchorynchus mykiss*) reported increases in respiration rates, mucous secretion, and edema in gill tissues, as well as erosion and fusion of intestinal villi.[13] Increases in intestinal Na^+K^+-ATPase activity and thiobarbituric acid reactive substances (TBARS) were also noted, most likely due to fish swallowing the SWCNTs. In a follow-up feeding study by the same group, similar effects were not observed and such variability may indicate the importance of exposure route in determining effects.[42] It is worth noting that in the current study and the aqueous exposure performed by Smith et al.,[13] fish were not fed throughout the duration of the study which may allow for more irritation of the intestinal tissue by SWCNTs compared to a food-borne exposure. Additionally, while the SWCNTs used in the current study and those used in the two previously mentioned studies shared similar characteristics, different dispersants were used to suspend the particles (gum arabic vs SDS) that have been shown to influence toxicological effects in aquatic organisms.[43] It is possible that the variable selection of dispersants contributes to some of the differential effects observed between studies. It should also be noted that the alteration in mucous cell morphology may not necessarily reflect a pathological response to SWCNTs and may in fact be a normal gut response to solid materials in general. Future studies to assess a food-born exposure route of SWCNTs will be informative in determining whether similar effects are observed under such scenarios.

Histological examination of proximal and distal sections of intestines revealed accumulation of mucin-encapsulated dark areas within the lumen of SWCNT-exposed animals which were not observed in association with the intestinal villi (Figure 3). Due to the absence of these areas in the controls (Figure 3A), it was assumed they represented large aggregates of SWCNTs (Figure 3B, 3C). TEM was used to delineate the presence of SWCNTs in the intestinal lumen (Figure 4). Though nanosized dense objects were observed, we were unable to confirm that they were SWCNTs, as similar structures were observed in some control images. Energy dispersive X-ray (EDX) spectroscopy was applied to attempt confirmation of the presence of SWCNTs indirectly by detection of the catalyst metals Mo and Co but this strategy proved to be unsuccessful (results not shown). These results are consistent with other studies, where identification of carbon

nanotubes using TEM in complex biological systems is ambiguous at best. For example, studies examining the distribution and effects of multiwalled carbon nanotubes (MWCNTs) in the African clawed frog (*Xenopus laevis*) positively identified materials in the intestines of the organisms using Raman spectroscopy, but could not discern dark masses within the intestinal tissues as MWCNTs.[44,45] Edgington et al.[15,46] examined the uptake and distribution of SWCNTs and MWCNTs in *Daphnia magna* using Raman, high resolution TEM, EDX, selective area diffraction, and electron energy loss spectroscopy. In these studies the authors were able to positively identify carbon nanomaterials within the intestinal lumen by Raman spectroscopy but dark areas within the intestinal tissue could not be confirmed as carbon particles and were identified as staining artifacts. The aforementioned studies collectively highlight the challenges associated with detection of carbon-based nanomaterials in vivo. In addition to the lack of specificity, time and resources required to perform nanoscale imaging limit the ability to evaluate material distribution in whole tissues.

In the current study, we were able to optimize a NIRF imaging technique to track SWCNTs in whole fish and organs. Immediately after gavage, SWCNT fluorescence was visible through the side of live fish tissue (Figure 5B vs Figure 5C) using NIRF imaging. As the gavage bolus dispersed in the intestinal tract over time, the ability to image the SWCNTs through lateral epidermal tissues decreased (Figure 5D). However, removal of the left filet revealed significant fluorescence that was contained in the intestinal tissue (Figure 5E). To further examine distribution, individual organs were dissected throughout the time series and NIRF images were collected. Liver, spleen, gall bladder, and reproductive organs did not show any significant SWCNT-derived NIRF fluorescence over time (images not shown), indicating no appreciable uptake through the intestinal epithelium. SWCNTs were only positively visualized in the intestines of the fish throughout the exposure (Figure 5H) and removal of all the organs in the body cavity eliminated fluorescence signal completely (Figure 5F). It is important to note that one major advantage of NIRF imaging for SWCNT detection is the extremely low background fluorescence in the near IR range inherent to most biological tissues. In our study of SWCNT distribution in fish with this technique, this low background conferred increased sensitivity of detection to our assay throughout the exposure time.

Image analysis of SWCNT-derived fluorescence in fish intestines was used to track residence time of the nanoparticles in the fish (Figure 6A), both visually and semiquantitatively. During the first 24 h following the exposure, the fluorescence appeared as a compact bolus that began to separate into smaller pockets and spread throughout the intestine at later time-points. We noted that under normal feeding conditions, fathead minnows package their intestinal contents as they move distally through the lumen which may explain development of these pockets as the SWNCTs traveled through the intestine. By 96 h, the majority of the SWCNTs had been excreted and by 168 h no SWCNTs were detected in the intestines as observed by the lack of fluorescence. Spatial fluorescence intensity maps were created (Figure 6B) based on individual pixel intensity which were used to semiquantify SWCNT fluorescence in intestinal images. Plotting average integrated fluorescence intensity of the images over time showed a trend consistent with our qualitative assessment of the images, that SWCNTs are excreted primarily within the first 24 h and then completely eliminated by 168 h post exposure (Figure 6C).

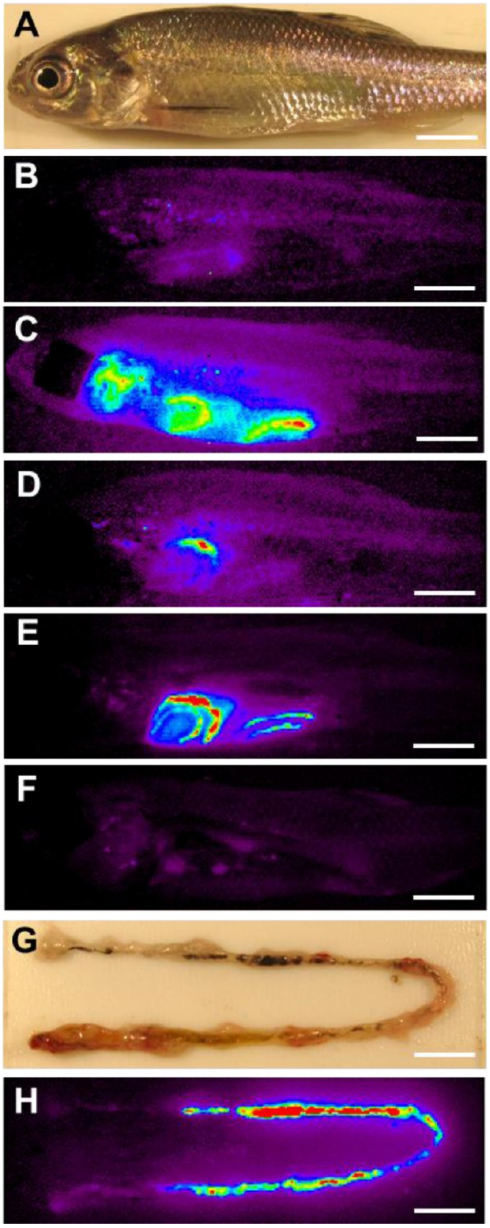

Figure 5. Near infrared fluorescence (NIRF) imaging for tracking SWCNTs in fish. Examples of fish images taken for a fish exposed via gavage for 8 h. (A) White light illuminated image of a fish is provided for reference. (B) NIRF image of a fish before gavage. (C) NIRF images of a fish immediately after gavage show strong fluorescence through depth of tissue which decreased dramatically after 8 h (D). Removal of left filet reveals strong fluorescence signal confined within the intestine (E). Removal of internal organs shows NIRF signal is also eliminated (F). Individualized intestines were imaged with white light for reference (G) and NIRF images were taken for tracking SWCNT distribution over time (H). Scale bars = 5 mm.

Quantitative analysis of SWCNT accumulation and depuration in intestines throughout the gavage exposure was conducted using a NIRF spectroscopic method (Figure 7) modified from previous studies.[25,26] Since the presence of intestinal tissue had a strong influence on recovery, a matrix-matched spike standard curve was used to quantify the SWCNTs. Initial recovery of gavage-spiked SWCNTs (0 h)

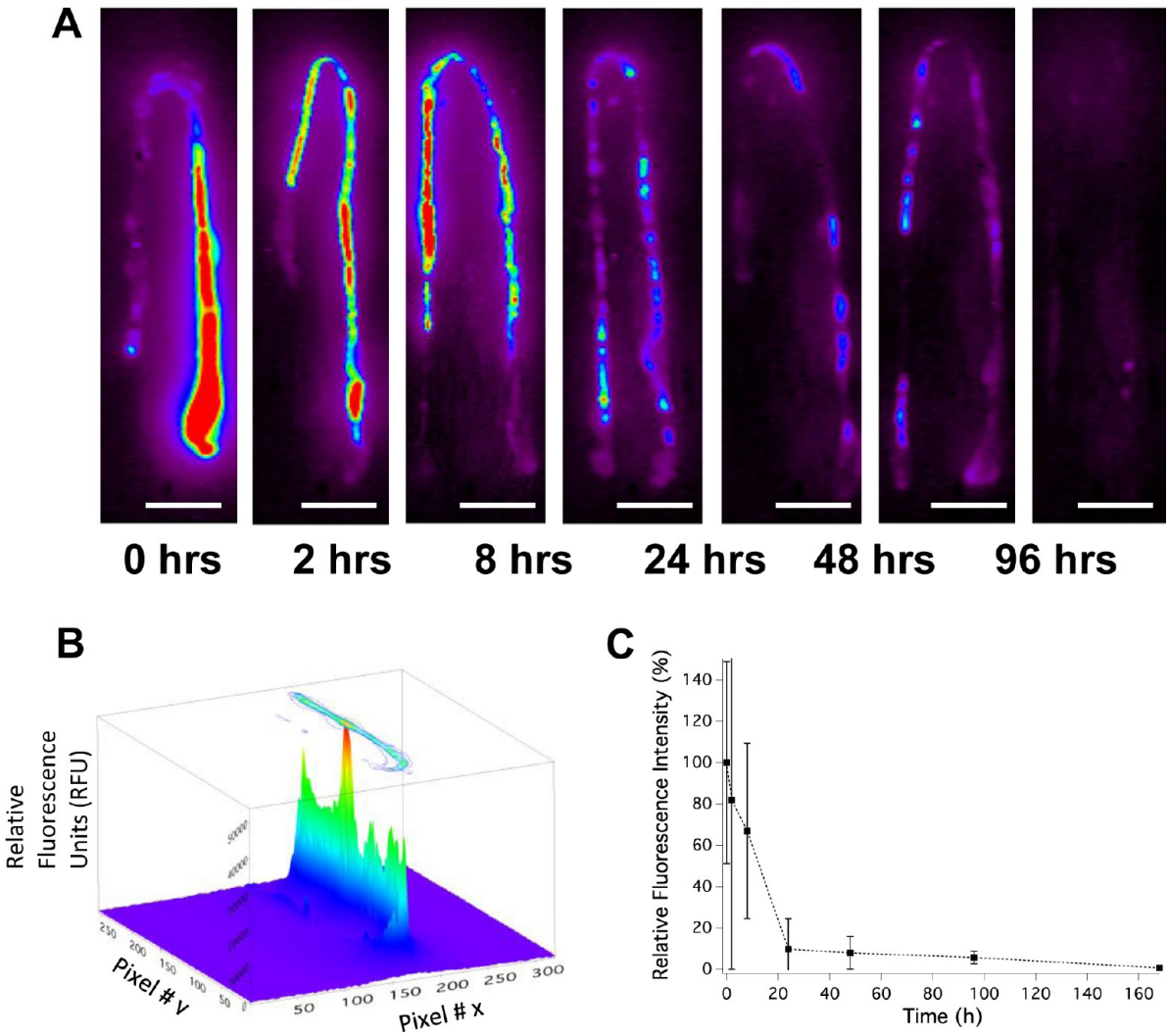

Figure 6. SWCNT residence time in fathead minnow intestines. (A) NIRF images of fish intestines over time demonstrate strong fluorescence after initial gavage decreasing over time with 168 h required for total excretion. Scale bars = 5 mm. (B) Image intensity was semiquantified using spatial fluorescence intensity mapping and (C) plotted over time for comparison to quantified intestine SWCNT burdens.

averaged 125% and declined over the remaining observation time following approximately first-order decay kinetics throughout the exposure until complete loss was observed at 168 h, yielding an estimated half-life of 27.1 ± 2.8 h. Comparison of SWCNT quantities measured in tissue (Figure 7) with the semiquantified images (Figure 6C) produced similar trends, indicating that both of these qualitative (imaging) and quantitative (spectroscopic) approaches can be used in conjunction to track and quantify SWCNTs in vivo. These techniques expand our ability to gain toxicological information regarding in vivo distribution of SWCNTs. The importance of our newly developed approach is highlighted in a recent report by Fraser et al.,[42] where the lack of validated techniques for examining broad distribution of SWCNTs in exposed fish limited their ability to determine if intestinal adsorption occurred.

While determining strict detection limits for our imaging system is difficult due to numerous factors influencing fluorescence (laser power, exposure time, tissue depth, dispersant, etc), using 10 μL of dilute suspensions we were able to detect as little as 0.75, 20, and 5 ng of SWCNTs in 2% SDC, 1% pluronic F68, and 0.5% gum arabic, respectively. Comparison of our NIRF images with our quantitative homogenate based NIRF spectroscopy method shows that at a minimum we can detect values at or below the detection limit (ng) of the quantitative method. We conclude that there was no appreciable uptake through the intestinal epithelium due to absence of fluorescence signal in the other organs examined during the exposure (liver, spleen, gall bladder, gonad) however, it is possible that very low concentrations of SWCNTs were present below our detection limits for both methods. In any case, the vast majority of SWCNTs remained confined in the intestines and were likely excreted by 168 h. Future studies performed with SWCNT mixed in a food matrix are warranted as this route of delivery may result in differential half-life and intestinal absorbance profiles.

Results of the current study demonstrate that NIRF can provide qualitative and quantitative assessment of SWCNT distribution in tissues with many advantages over other techniques that have been used to examine SWCNTs in environmental matrices. Techniques such as TEM require a high level of expertise, can be cost and time prohibitive, and lack adequate protocol for positive identification of carbon nanomaterials in tissues.[15] Other approaches, such as

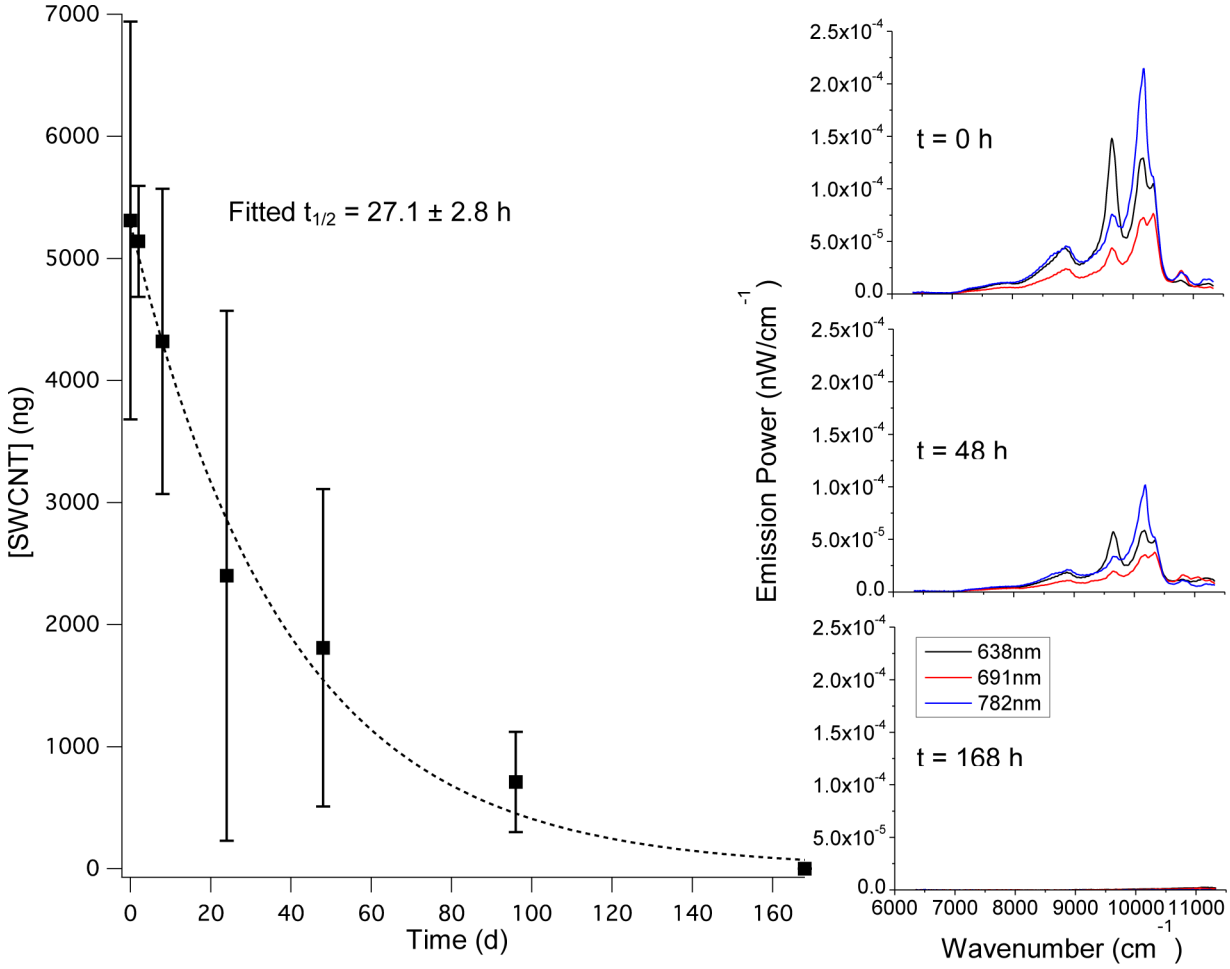

Figure 7. SWCNT mass in fish intestines as measured using NIRF spectroscopy. Representative NIRF spectra are shown for three time points to the left. Half life of the SWCNT burdens within fish intestines were modeled over the experiment time using first-order decay kinetics, yielding an estimated half-life of 27.1 ± 2.8 h.

fluorescent tagging of carbon nanomaterials, have been employed for in vivo tracking;[47,48] however, the potential for enzymatic cleavage of the tag, background endogenous fluorescence, and alteration of biological uptake kinetics limit the usefulness of such techniques.[27] Radioactive labeling of carbon nanomaterials has also been used, which requires customized synthesis, additional purification, and can also be cost prohibitive.[25,49] Although Raman spectroscopy has been shown to be effective in identifying SWCNTs in some systems, it lacks the sensitivity necessary for detection at low concentrations in biological samples.[15] Major advantages of NIRF imaging thus include: no requirement for tagging of semiconducting SWCNTs, ability to image whole live organisms that can be dissected with no special preparation, and ease of operation and rapid evaluation of samples.

In the current study we have demonstrated that our NIRF technique is highly sensitive, with little endogenous background fluorescence and possess low detection limits. Parallel measurements using semiquantitative NIRF and spectroscopy-based NIRF quantitation methods showed comparable trends, indicating accuracy of the technique in detecting semiconducting SWCNTs live fish samples. To date, NIRF has been successfully used to analyze SWCNTs in aqueous environmental samples, sediment, invertebrates, and now fish tissues. This study highlights the applicability of NIRF for SWCNT detection in aquatic environmental and toxicological studies.

■ AUTHOR INFORMATION

Corresponding Author

*Phone: (352)294-5293; e-mail: sabo@phhp.ufl.edu.

Present Addresses

◆(J.A.M.) Department of Chemistry and Physics, Arkansas State University, P.O. Box 419, State University, Arkansas 72467, United States.

¶(A.N.P.) Atlantic Ecology Division, U.S. Environmental Protection Agency, 27 Tarzwell Drive, Narragansett, Rhode Island 02882, United States.

□(A.R.M.N.A. and N.B.S.) Department of Civil, Architectural and Environmental Engineering University of Texas at Austin 301 E. Dean Keeton Street ECJ 8.608 Austin, Texas 78712.

Author Contributions

The manuscript was written through contributions of all authors. All authors have given approval to the final version of the manuscript.

Notes

The authors declare no competing financial interest.

■ ACKNOWLEDGMENTS

We thank the following undergraduate and graduate students who assisted with some of the experiments: B. Castillo, M. L. Morris, S. Ponavolu, L.C. Smith, C. Lavelle, and M. Ali. H. Dai and G. Hong deserve our gratitude for inviting us to examine their NIR imaging system as an example when building our own. We also thank P. Wallis (SouthWest NanoTechnologies) for providing SWCNT materials for this experiment. We thank the National Science Foundation (Grant No. 0933484 to N.B.S and Grant No. 1236029 to T.S.A) as well as the U.S. Environmental Protection agency (Grant No. RD833859 to P.L.F.) for funding.

■ ABBREVIATIONS

SWCNT	single-walled carbon nanotube
TEM	transmission electron microscopy
MWCNT	multiwalled carbon nanotube
EDS	energy dispersive X-ray spectroscopy
NIRF	near infrared fluorescence

■ REFERENCES

(1) Niyogi, S.; Hamon, M.; Hu, H.; Zhao, B.; Bhowmik, P.; Sen, R.; Itkis, M.; Haddon, R. Chemistry of single-walled carbon nanotubes. *Acc. Chem. Res.* **2002**, *35*, 1105−1113.

(2) Templeton, R. C.; Ferguson, P. L.; Washburn, K. M.; Scrivens, W. A.; Chandler, G. T. Life-cycle effects of single-walled carbon nanotubes (SWNTs) on an estuarine meiobenthic copepod. *Environ. Sci. Technol.* **2006**, *40*, 7387−7393.

(3) Lam, C.; James, J.; McCluskey, R.; Arepalli, S.; Hunter, R. A review of carbon nanotube toxicity and assessment of potential occupational and environmental health risks. *Crit. Rev. Toxicol.* **2006**, *36*, 189−217.

(4) Andujar, P.; Lanone, S.; Brochard, P.; Boczkowski, J. Respiratory effects of manufactured nanoparticles. *Rev. Mal. Respir.* **2011**, *28*, e66−e75.

(5) Castranova, V. Overview of current toxicological knowledge of engineered nanoparticles. *J. Occup. Environ. Med.* **2011**, *53*, S14−S17.

(6) Bonner, J. C. Nanoparticles as a potential cause of pleural and interstitial lung disease. *Proc. Am. Thorac. Soc.* **2010**, *7*, 138.

(7) Kang, S.; Mauter, M. S.; Elimelech, M. Microbial cytotoxicity of carbon-based nanomaterials: Implications for river water and wastewater effluent. *Environ. Sci. Technol.* **2009**, *43*, 2648−2653.

(8) Roberts, A. P.; Mount, A. S.; Seda, B.; Souther, J.; Qiao, R.; Lin, S.; Ke, P. C.; Rao, A. M.; Klaine, S. J. In vivo biomodification of lipid-coated carbon nanotubes by *Daphnia magna*. *Environ. Sci. Technol.* **2007**, *41*, 3025−3029.

(9) da Rocha, A. M.; Ferreira, J. R.; Barros, D. M.; Brandao Pereira, T. C.; Bogo, M. R.; Oliveira, S.; Geraldo, V.; Lacerda, R. G.; Ferlauto, A. S.; Ladeira, L. O.; Brant Pinheiro, M. V.; Monserrat, J. M. Gene expression and biochemical responses in brain of zebrafish *Danio rerio* exposed to organic nanomaterials: Carbon nanotubes (SWCNT) and fullerenol (C-60(OH)(18−22)(OK4)). *Comp. Biochem. Physiol., Part A: Mol. Integr. Physiol.* **2013**, *165*, 460−467.

(10) Thomas, K. V.; Farkas, J.; Farmen, E.; Christian, P.; Langford, K.; Wu, Q.; Tollefsen, K. Effects of Dispersed Aggregates of Carbon and Titanium Dioxide Engineered Nanoparticles on Rainbow Trout Hepatocytes. *J. Toxicol. Environ. Health, Part A* **2011**, *74*, 466−477.

(11) Klaper, R.; Arndt, D.; Setyowati, K.; Chen, J.; Goetz, F. Functionalization impacts the effects of carbon nanotubes on the immune system of rainbow trout, *Oncorhynchus mykiss*. *Aquat. Toxicol.* **2010**, *100*, 211−217.

(12) Cheng, J.; Flahaut, E.; Cheng, S. H. Effect of carbon nanotubes on developing zebrafish (*Danio rerio*) embryos. *Environ. Toxicol. Chem.* **2007**, *26*, 708−716.

(13) Smith, C. J.; Shaw, B. J.; Handy, R. D. Toxicity of single walled carbon nanotubes to rainbow trout, (*Oncorhynchus mykiss*): Respiratory toxicity, organ pathologies, and other physiological effects. *Aquatic Toxicology* **2007**, *82*, 94−109.

(14) Simonet, B. M.; Valcarcel, M. Monitoring nanoparticles in the environment. *Anal. Bioanal. Chem.* **2009**, *393*, 17−21.

(15) Edgington, A.; Petersen, E. J.; Herzing, A. A.; Podila, R.; Rao, A.; Klaine, S. J. Microscopic investigation of single-wall carbon nanotube uptake by *Daphnia magna*. *Nanotox* **2013**, DOI: 10.3109/17435390.2013.847504.

(16) Alpatova, A. L.; Shan, W.; Babica, P.; Upham, B. L.; Rogensues, A. R.; Masten, S. J.; Drown, E.; Mohanty, A. K.; Alocilja, E. C.; Tarabara, V. V. Single-walled carbon nanotubes dispersed in aqueous media via non-covalent functionalization: Effect of dispersant on the stability, cytotoxicity, and epigenetic toxicity of nanotube suspensions. *Water Res.* **2010**, *44*, 505−520.

(17) Bauer, B. J.; Becker, M. L.; Bajpai, V.; Fagan, J. A.; Hobbie, E. K.; Migler, K.; Guttman, C. M.; Blair, W. R. Measurement of single-wall nanotube dispersion by size exclusion chromatography. *J. Phys. Chem. C* **2007**, *111*, 17914−17918.

(18) Jaisi, D. P.; Saleh, N. B.; Blake, R. E.; Elimelech, M. Transport of single-walled carbon nanotubes in porous media: Filtration mechanisms and reversibility. *Environ. Sci. Technol.* **2008**, *42*, 8317−8323.

(19) Plata, D. L.; Reddy, C. M.; Gschwend, P. M. Thermogravimetry-mass spectrometry for carbon nanotube detection in complex mixtures. *Environ. Sci. Technol.* **2012**, *46*, 12254−12261.

(20) Baughman, R.; Zakhidov, A.; de Heer, W. Carbon nanotubes—The route toward applications. *Science* **2002**, *297*, 787−792.

(21) O'Connell, M.; Bachilo, S.; Huffman, C.; Moore, V.; Strano, M.; Haroz, E.; Rialon, K.; Boul, P.; Noon, W.; Kittrell, C.; Ma, J.; Hauge, R.; Weisman, R.; Smalley, R. Band gap fluorescence from individual single-walled carbon nanotubes. *Science* **2002**, *297*, 593−596.

(22) Bachilo, S.; Strano, M.; Kittrell, C.; Hauge, R.; Smalley, R.; Weisman, R. Structure-assigned optical spectra of single-walled carbon nanotubes. *Science* **2002**, *298*, 2361−2366.

(23) Frangioni, J. In vivo near-infrared fluorescence imaging. *Curr. Opin. Chem. Biol.* **2003**, *7*, 626−634.

(24) Robinson, J. T.; Hong, G.; Liang, Y.; Zhang, B.; Yaghi, O. K.; Dai, H. In vivo fluorescence imaging in the second near-infrared window with long circulating carbon nanotubes capable of ultrahigh tumor uptake. *J. Am. Chem. Soc.* **2012**, *134*, 10664−10669.

(25) Schierz, A.; Parks, A. N.; Washburn, K. M.; Chandler, G. T.; Ferguson, P. L. Characterization and quantitative analysis of single-walled carbon nanotubes in the aquatic environment using near-infrared fluorescence spectroscopy. *Environ. Sci. Technol.* **2012**, *46*, 12262−12271.

(26) Parks, A. N.; Portis, L. M.; Schierz, P. A.; Washburn, K. M.; Perron, M. M.; Burgess, R. M.; Ho, K. T.; Chandler, G. T.; Ferguson, P. L. Bioaccumulation and toxicity of single-walled carbon nanotubes to benthic organisms at the base of the marine food chain. *Environ. Toxicol. Chem.* **2013**, *32*, 1270−1277.

(27) Cherukuri, P.; Bachilo, S.; Litovsky, S.; Weisman, R. Near-infrared fluorescence microscopy of single-walled carbon nanotubes in phagocytic cells. *J. Am. Chem. Soc.* **2004**, *126*, 15638−15639.

(28) Welsher, K.; Liu, Z.; Daranciang, D.; Dai, H. Selective probing and imaging of cells with single walled carbon nanotubes as near-infrared fluorescent molecules. *Nano Lett.* **2008**, *8*, 586−590.

(29) Leeuw, T. K.; Reith, R. M.; Simonette, R. A.; Harden, M. E.; Cherukuri, P.; Tsyboulski, D. A.; Beckingham, K. M.; Weisman, R. B. Single-walled carbon nanotubes in the intact organism: Near-IR imaging and biocompatibility studies in Drosophila. *Nano Lett.* **2007**, *7*, 2650−2654.

(30) Welsher, K.; Liu, Z.; Sherlock, S. P.; Robinson, J. T.; Chen, Z.; Daranciang, D.; Dai, H. A route to brightly fluorescent carbon nanotubes for near-infrared imaging in mice. *Nat. Nanotechnol.* **2009**, *4*, 773−780.

(31) Welsher, K.; Sherlock, S. P.; Dai, H. Deep-tissue anatomical imaging of mice using carbon nanotube fluorophores in the second near-infrared window. *Proc. Natl. Acad. Sci. U. S. A.* **2011**, *108*, 8943−8948.

(32) Nowack, B.; Bucheli, T. D. Occurrence, behavior and effects of nanoparticles in the environment. *Environ. Pollut.* **2007**, *150*, 5−22.
(33) Afrooz, A. R. M. N.; Khan, I. A.; Hussain, S. M.; Saleh, N. B. Mechanistic heteroaggregation of gold nanoparticles in a wide range of solution chemistry. *Environ. Sci. Technol.* **2013**, *47*, 1853−1860.
(34) Khan, I. A.; Afrooz, A. R. M. N.; Flora, J. R. V.; Schierz, P. A.; Ferguson, P. L.; Sabo-Attwood, T.; Saleh, N. B. Chirality affects aggregation kinetics of single-walled carbon nanotubes. *Environ. Sci. Technol.* **2013**, *47*, 1844−1852.
(35) Khan, I. A.; Aich, N.; Afrooz, A.; Flora, J. R.; Schierz, P. A.; Ferguson, P. L.; Sabo-Attwood, T.; Saleh, N. B. Fractal structures of single-walled carbon nanotubes in biologically relevant conditions: Role of chirality vs. media conditions. *Chemosphere* **2013**, *93*, 1997−2003.
(36) Prophet, E. B.; Mills, B.; Arrington, J. B.; Sobin, L. H. *Laboratory Methods in Histotechnology*; American Registry of Pathology: Washington, DC, 1992.
(37) Handy, R. D.; Al-Bairuty, G.; Al-Jubory, A.; Ramsden, C. S.; Boyle, D.; Shaw, B. J.; Henry, T. B. Effects of manufactured nanomaterials on fishes: A target organ and body systems physiology approach. *J. Fish Biol.* **2011**, *79*, 821−853.
(38) Loiseau, A.; Gavillet, J.; Ducastelle, F.; Thibault, J.; Stéphan, O.; Bernier, P.; Thair, S. Nucleation and growth of SWNT: TEM studies of the role of the catalyst. *C. R. Phys.* **2003**, *4*, 975−991.
(39) Kimball, G. L. *The Effects of Lesser Known Metals and One Organic to Fathead Minnows (Pimephales promelas) and Daphnia magna*; Department of Entomology, Fisheries and Wildlife, University of Minnesota, Minneapolis, MN1978; Unpublished Manuscript
(40) Ju, L.; Zhang, W.; Wang, X.; Hu, J.; Zhang, Y. Aggregation kinetics of SDBS-dispersed carbon nanotubes in different aqueous suspensions. *Colloids Surf., A* **2012**, *409*, 159−166.
(41) Saleh, N. B.; Pfefferle, L. D.; Elimelech, M. Influence of biomacromolecules and humic acid on the aggregation kinetics of single-walled carbon nanotubes. *Environ. Sci. Technol.* **2010**, *44*, 2412−2418.
(42) Fraser, T. W. K.; Reinardy, H. C.; Shaw, B. J.; Henry, T. B.; Handy, R. D. Dietary toxicity of single-walled carbon nanotubes and fullerenes (C-60) in rainbow trout (*Oncorhynchus mykiss*). *Nanotoxicology* **2011**, *5*, 98−108.
(43) Gao, J.; Llaneza, V.; Youn, S.; Silvera-Batista, C. A.; Ziegler, K. J.; Bonzongo, J. J. Aqueous suspension methods of carbon-based nanomaterials and biological effects on model aquatic organisms. *Environ. Toxicol. Chem.* **2012**, *31*, 210−214.
(44) Flahaut, E.; Gauthier, L.; Landois, P.; Mouchet, F.; Pinelli, E.; Puech, P. Carbon nanotube ecotoxicity in amphibians: Assessment of multiwalled carbon nanotubes and comparison with double-walled carbon nanotubes. *Nanomedicine* **2010**, *5*, 963+.
(45) Mouchet, F.; Landois, P.; Sarremejean, E.; Bernard, G.; Puech, P.; Pinelli, E.; Flahaut, E.; Gauthier, L. Characterisation and in vivo ecotoxicity evaluation of double-wall carbon nanotubes in larvae of the amphibian. *Aquat. Toxicol.* **2008**, *87*, 127−137.
(46) Edgington, A. J.; Roberts, A. P.; Taylor, L. M.; Alloy, M. M.; Reppert, J.; Rao, A. M.; Mao, J.; Klaine, S. J. The influence of natural organic matter on the toxicity of multiwalled carbon nanotubes. *Environ. Toxicol. Chem.* **2010**, *29*, 2511−2518.
(47) Shi Kam, N. W.; Jessop, T. C.; Wender, P. A.; Dai, H. Nanotube molecular transporters: Internalization of carbon nanotube-protein conjugates into mammalian cells. *J. Am. Chem. Soc.* **2004**, *126*, 6850−6851.
(48) Pantarotto, D.; Briand, J.; Prato, M.; Bianco, A. Translocation of bioactive peptides across cell membranes by carbon nanotubes. *Chem. Commun.* **2004**, 16−17.
(49) Petersen, E. J.; Akkanen, J.; Kukkonen, J. V.; Weber, W. J., Jr. Biological uptake and depuration of carbon nanotubes by *Daphnia magna*. *Environ. Sci. Technol.* **2009**, *43*, 2969−2975.